Journal of Power Sources 250 (2014) 313–318

Contents lists available at ScienceDirect

Journal of Power Sources

journal homepage: www.elsevier.com/locate/jpowsour

Interface modifications by anion receptors for high energy lithium ion batteries

Jianming Zheng [a], Jie Xiao [a,*], Meng Gu [b], Pengjian Zuo [a], Chongmin Wang [b], Ji-Guang Zhang [a,*]

[a] Energy and Environmental Directorate, Pacific Northwest National Laboratory, 902 Battelle Boulevard, Richland, WA 99352, USA
[b] Environmental Molecular Science Laboratory, Pacific Northwest National Laboratory, 902 Battelle Boulevard, Richland, WA 99352, USA

HIGHLIGHTS

- TPFPB coordinates with active oxygen species released from structural lattice.
- Side reactions between oxygen species and carbonate-based electrolyte are reduced.
- Dissolution of oxygen in TPFPB added electrolyte reduces its exposure to carbonate solvents.
- Insulating salts LiF/Li_2O derived from electrolyte decomposition are soluble in TPFPB.
- The growth of passivation film on cathode surface is slowed down.

GRAPHICAL ABSTRACT

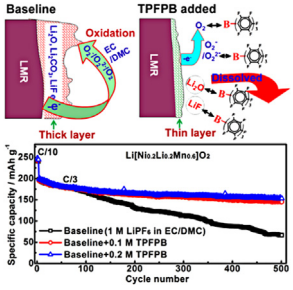

ARTICLE INFO

Article history:
Received 26 July 2013
Received in revised form
4 October 2013
Accepted 10 October 2013
Available online 9 November 2013

Keywords:
Anion receptor
Electrolyte additive
Layered composite cathode
Cycling stability
Lithium-ion batteries

ABSTRACT

Li-rich, Mn-rich (LMR) layered composite has attracted extensive interests because of its highest energy density among all cathode candidates for lithium ion batteries (LIB). However, capacity degradation and voltage fading remain the major challenges for LMR cathodes prior to their practical applications. Here, we demonstrate that anion receptor, tris(pentafluorophenyl)borane ($(C_6F_5)_3B$, TPFPB), substantially enhances the stability of electrode/electrolyte interface and thus improves the cycling stability of LMR cathode $Li[Li_{0.2}Ni_{0.2}Mn_{0.6}]O_2$. In the presence of 0.2 M TPFPB, $Li[Li_{0.2}Ni_{0.2}Mn_{0.6}]O_2$ shows an improved capacity retention of 76.8% after 500 cycles. It is proposed that TPFPB effectively confines the highly active oxygen species released from structural lattice through its strong coordination ability and high oxygen solubility. The electrolyte decomposition caused by the oxygen species attack is therefore largely mitigated, forming reduced amount of byproducts on the cathode surface. Additionally, other salts such as insulating LiF derived from electrolyte decomposition are also soluble in the presence of TPFPB. The collective effects of TPFPB mitigate the accumulation of parasitic reaction products and stabilize the interfacial resistances between cathode and electrolyte during extended cycling, thus significantly improving the cycling performance of $Li[Li_{0.2}Ni_{0.2}Mn_{0.6}]O_2$.

1. Introduction

Development of high-energy cathode materials is critical for advanced lithium ion batteries that can be deployed for vehicle electrification [1–4]. Compared to the traditional cathodes such as $LiMn_2O_4$ spinel and layered $LiCoO_2$, the series of Li-rich, Mn-

* Corresponding authors. Tel.: +1 509 375 4598; fax: +1 509 372 2186.
E-mail addresses: Jie.xiao@pnnl.gov, jxiao1980@gmail.com (J. Xiao), Jiguang.zhang@pnnl.gov (J.-G. Zhang).

0378-7753/$ – see front matter © 2013 Elsevier B.V. All rights reserved.
http://dx.doi.org/10.1016/j.jpowsour.2013.10.071

rich (LMR) layered composites, $xLi_2MnO_3 \cdot (1-x)\ LiMO_2$ (M = Ni, Co, Mn, $0 \leq x \leq 1$), have so far demonstrated the highest discharge capacity along with cost reduction and safety enhancement [3,4]. The advantages of Li_2MnO_3 component and its influence on the structural stability and electrochemical properties of these LMR cathode series have been extensively investigated by many research groups [3–9]. After activation of Li_2MnO_3 in the initial charge process, a discharge capacity of greater than 250 mAh g^{-1} can be achieved for these layered composite cathodes. However, oxygen is simultaneously released during Li_2MnO_3 activation, resulting in the damage of electrode surface structure, formation of micro-cracks at the crystal surface and the distortion of crystal periodicity [10–12]. More importantly, the extracted intermediate oxygen species (e.g. O_2^{2-}, O_2^- or even $O_2^{\bullet-}/O^{\bullet-}$) steadily oxidize the organic solvents and form passivation film on the cathode [13]. Similar phenomena were extensively reported in Li–O_2 batteries employing alkyl carbonate electrolytes [14,15]. In addition, high cut-off voltage (4.6–4.8 V) beyond the stability of carbonate-based electrolyte is required for LMR cathode and unavoidably initiates electrolyte decomposition during each charge, further thickening the passivation layer on the cathode surface and deteriorating the electrochemical performances of LMR cathodes [5,16–20].

In this work, boron-based anion receptor, tris(pentafluorophenyl)borane (TPFPB) was adopted as an electrolyte additive to limit the negative effects from oxygen species in the system. TPFPB was ever reported to improve the performances of batteries containing graphite and $LiMn_2O_4$ by partially dissolving the byproducts such as LiF and Li_2O [21–25]. Considering the strong anion coordination effect of TPFPB, the released oxygen species in the form of oxygen anions (O_2^{2-}/O_2^-) or radicals ($O_2^{\bullet-}/O^{\bullet-}$) may be trapped in the vicinity of TPFPB instead of attacking the electrolyte. Based on this hypothesis, a systematic investigation was performed in this work to verify this concept which may provide valuable clues to guide the research and development of electrolyte additives to modify the interfacial reactions.

2. Experimental

2.1. Electrode and electrolyte preparation

$Li[Li_{0.2}Ni_{0.2}Mn_{0.6}]O_2$ was prepared by a co-precipitation method [19,26]. Nickel sulfate hexahydrate ($NiSO_4 \cdot 6H_2O$), manganese sulfate monohydrate ($MnSO_4 \cdot H_2O$), sodium hydroxide (NaOH), were used as the starting materials to prepare $Ni_{0.25}Mn_{0.75}(OH)_2$ precursor. The precursor material was washed with deionized (DI) water to remove residual sodium and sulfate species, then filtered and dried inside a vacuum oven set at 120 °C overnight. $Ni_{0.25}Mn_{0.75}(OH)_2$ was well mixed with Li_2CO_3 and then calcined at 900 °C for 24 h to obtain the cathode materials. The baseline electrolyte was prepared by dissolving 1 M lithium hexafluorophosphate ($LiPF_6$) in ethyl carbonate (EC) and dimethyl carbonate (DMC) (1:2 in volume), while TPFPB (from Aldrich) added electrolyte was prepared by dissolving 1 M $LiPF_6$ and 0.1/0.2 mol TPFPB in EC/DMC solvents. The viscosity measurement was conducted on a Brookfield DV-II + Pro Cone/Plate Viscometer and the conductivity was measured by an Oakton® 650 Series Multiparameter Meter [27]. Before tests, all apparatuses were calibrated and the electrolytes were maintained at 25 °C in a constant temperature oil bath (Brookfield Circulating Bath Model TC-502). Transmission Electron Microscopy (TEM) was analyzed using a probe-aberration corrected FEI Titan STEM and image-corrected FEI ETEM at 300 kV.

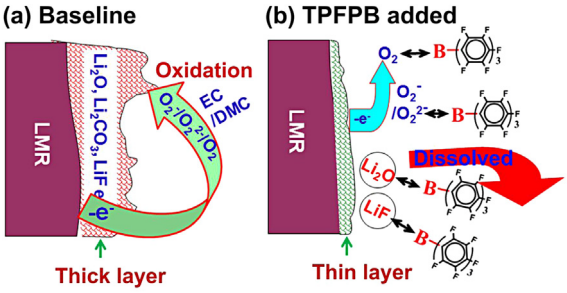

Fig. 1. Scheme of the functioning mechanism of TPFPB. (a) Thick passivation layer formation in baseline electrolyte; (b) significantly reduced passivation layer formation in TPFPB added electrolyte.

2.2. Electrochemical performance measurements

Cathode electrodes were prepared by coating a slurry containing 80% $Li[Li_{0.2}Ni_{0.2}Mn_{0.6}]O_2$, 10% super P (from Timcal), and 10% poly(vinylidene fluoride) (PVDF, Kynar HSV900, Arkema Inc.) binder onto Al current collector foil. After drying, the electrodes were punched into disks with ø = 1.27 cm. A typical loading of the cathode electrode is about 3 mg cm^{-2}. Coin cells were assembled with the cathode electrodes as-prepared, metallic lithium foil as counter electrode, Celgard K1640 monolayer polyethylene membrane as separator and carbonate-based electrolyte in an argon-filled MBraun glove box. Same amount of electrolyte of 100 μL was used for coin-cell assembly. The electrochemical performance measurements were performed galvanostatically between 2.0 and 4.7 V at C/3 (1 C = 250 mA g^{-1}) after three formation cycles at C/10 on an Arbin BT-2000 battery tester at room temperature (~25 °C). Oxidation potentials of the electrolytes without and with TPFPB additive were measured using Pt as working electrode and Li metal as both counter and reference electrodes in a three-electrode cell. Electrochemical impedance spectra (EIS) measurements were performed using a CHI 6005D electrochemical station (CH Instruments) in a frequency range from 100 kHz to 10 mHz with a perturbation amplitude of ±10 mV.

3. Results and discussion

Tris(pentafluorophenyl)borane (TPFPB) is one of the exemplar anion receptors based on electron deficient borate or borane compounds with different fluorinated aryl or alkyl groups. Because of the electron deficient boron and relative inertness of the B–C bonds, TPFPB is considered to be an effective anion receptor and usually used to improve the dissolution of various lithium salts including LiF, Li_2O_2 and Li_2O, that are basically insoluble in organic solvents [28–30]. Perfluorotributylamine (FTBA) with similar empty orbitals on nitrogen atoms was reported to promote O_2 solubility even in carbonate-based electrolyte, functioning as O_2 carrier in lithium oxygen batteries [31]. However, solubility of FTBA is quite limited in conventional EC/DMC based electrolyte, thus TPFPB is used in this work to prove the concept of using anion receptor as additive to modify the interfacial reactions on LMR cathode surface.

The working mechanism of TPFPB is proposed in Fig. 1. During the activation of Li_2MnO_3 component, oxygen is extracted out of the structural lattice as highly active oxygen species, e.g. O_2^-/O_2^{2-}, or $O_2^{\bullet-}/O^{\bullet-}$, which are reactive Lewis base that could readily decompose the carbonate-based electrolyte [5]. It is hypothesized that O_2^-/O_2^{2-} extracted out of LMR lattice can be partially captured by boron atom located in the center of TPFPB instead of direct exposure to the electrolyte to initiate parasitic reactions

Table 1
Physical properties of the electrolyte solutions.

	Baseline electrolyte	0.1 M TPFPB added	0.2 M TPFPB added
Conductivity/ mS cm^{-1}	11.65	9.93	8.59
Viscosity/cp	3.35	3.89	4.40

around cathode. Even though O_2 still forms, it dissolves in the presence of TPFPB since the oxygen solubility in perfluorinated compound is much higher than in carbonate solvents [32]. The byproducts derived from the interactions between electrolyte and O_2^-/O_2^{2-} are therefore substantially reduced. Other parasitic reactions such as electrolyte decomposition at high voltages also produce insulating salts such as LiF and Li_2O etc., which are again soluble in the presence of TPFPB [33]. Therefore, the intensive interfacial reactions during the first cycle as well as the continuous accumulation of passivation film on cathode surface are significantly alleviated in the presence of TPFPB, which stabilizes the electrode/electrolyte interface. Of note, the PF_6^- anions of lithium salt $LiPF_6$ in the electrolyte may also coordinate with TPFPB. However, PF_6^- has much poorer coordination ability as compared to F^- and O^{2-} [34]. Therefore, most of O-species once generated and insoluble byproduct LiF will still be effectively captured by TPFPB as proposed in this work.

Table 1 shows that the electrolyte conductivity decreases while the viscosity increases with increasing TPFPB (solid state at room temperature) content in the electrolyte. Fig. 2 is the typical cyclic voltammograms (CV) for the electrolytes without and with TPFPB additive, which were recorded on Pt electrode over 3.0–6.0 V at a scan rate of 1 mV s^{-1}. TPFPB additive is stable up to ca. 5.0 V, comparable to 1 M $LiPF_6$ in EC/DMC and consistent with the literature report [28].

Fig. 3a shows the initial charge–discharge curves of Li$[Li_{0.2}Ni_{0.2}Mn_{0.6}]O_2$ in electrolytes with different TPFPB concentrations between 2.0 and 4.7 V. The charge/discharge profiles almost overlap with each other for Li$[Li_{0.2}Ni_{0.2}Mn_{0.6}]O_2$ electrodes in baseline electrolyte and TPFPB added electrolyte due to the low current density (C/10) used for the first three formation cycles. An irreversible voltage plateau at ca. 4.4–4.6 V is observed in all three cells caused by the lithium ion removal concomitant with irreversible loss of oxygen from the LMR electrode lattice [5,7,35]. After activation, the electrode material delivers similarly high discharge capacity of ca. 245 mAh g^{-1} in all electrolytes

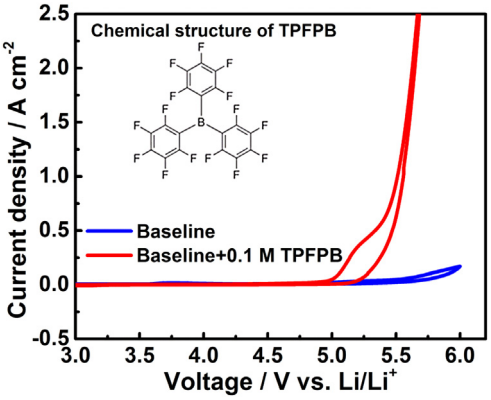

Fig. 2. The cyclic voltammograms (CV) for the electrolytes without and with TPFPB additive recorded on Pt electrode at a scan rate of 1 mV s^{-1}. The inset shows the chemical structure of TPFPB.

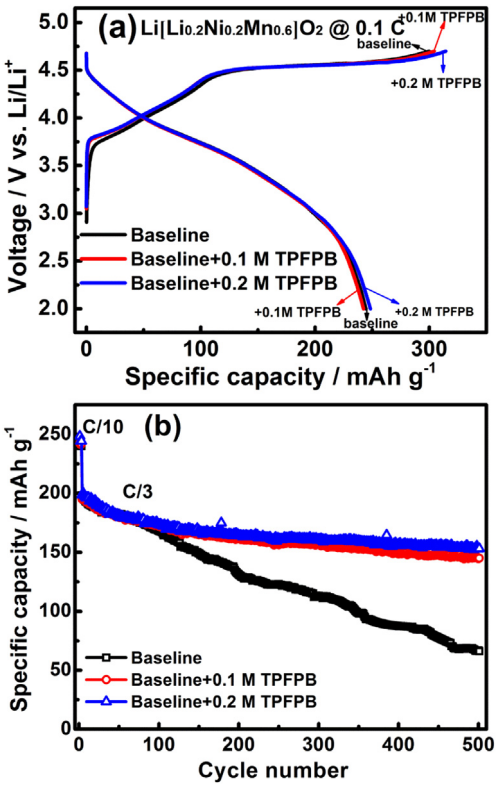

Fig. 3. (a) Initial charge/discharge profiles at C/10 (25 mA g^{-1}) and (b) long-term cycling performance of cathode material Li$[Li_{0.2}Ni_{0.2}Mn_{0.6}]O_2$ at C/3 after three formation cycles at C/10.

(Fig. 3a), indicating that TPFPB additive has good compatibility with both Li$[Li_{0.2}Ni_{0.2}Mn_{0.6}]O_2$ electrode and the electrolyte during electrochemical processes. In the subsequent cycling at C/3 (Fig. 3b), an initial discharge capacity of ~200 mAh g^{-1} was

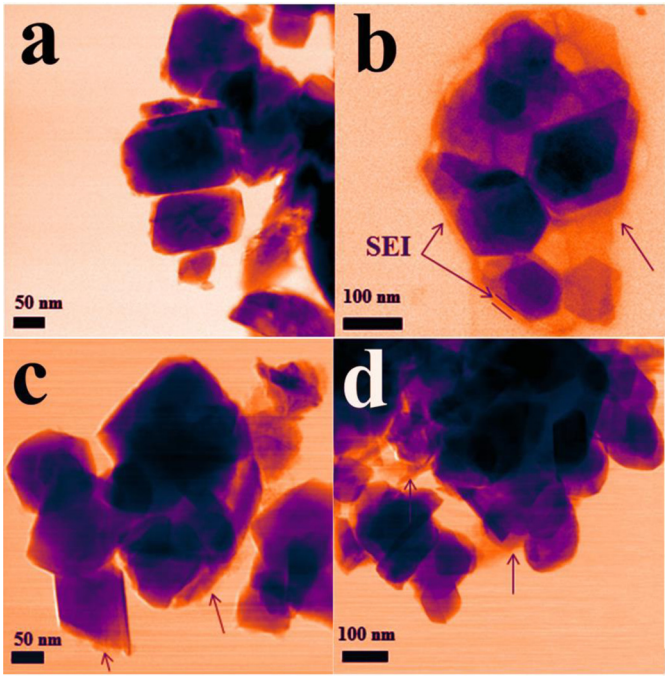

Fig. 4. TEM images of fresh electrode and electrodes cycled in electrolytes without and with TPFPB additive after 300 cycles at C/3. (a) Fresh, (b) baseline, (c) 0.1 M TPFPB, (d) 0.2 M TPFPB.

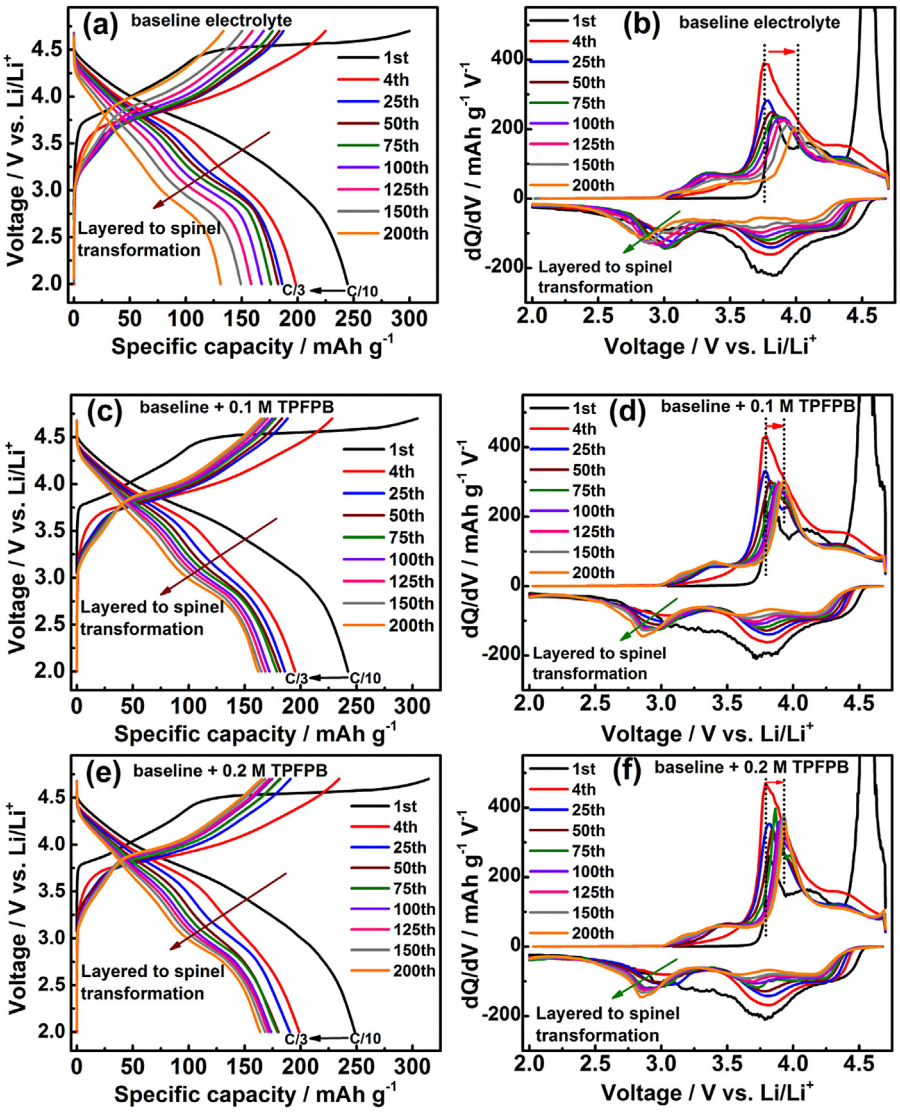

Fig. 5. Charge/discharge profiles and corresponding dQ/dV curves of cathode material $Li[Li_{0.2}Ni_{0.2}Mn_{0.6}]O_2$ in (a, b) baseline electrolyte, (c, d) 0.1 M TPFPB added electrolyte, and (e, f) 0.2 M TPFPB added electrolyte.

still achieved in all cells. However, fast capacity fading was observed for $Li[Li_{0.2}Ni_{0.2}Mn_{0.6}]O_2$ in baseline electrolyte upon cycling, which retains only 33.5% of its initial capacity after 500 cycles. In contrast, remarkably improved cycling stability is revealed with the addition of TPFPB. Even after 500 cycles, the discharge capacities were maintained at 145 and 153 mAh g^{-1} for cathodes tested in electrolytes with 0.1 M and 0.2 M TPFPB, respectively, corresponding to high capacity retentions of 74.2% and 76.8%, which are among of the best performances ever reported for LMR cathode materials. For LMR cathode, one important reason for the continuous capacity fading is the deterioration of electrode/electrolyte interface, associated with the thick passivation layer formation and the corrosion/fragmentation of LMR cathode bulk structure [5,12,36]. If TPFPB in the electrolyte effectively accepts oxygen anions or radicals before O_2 is generated, the damages to surface structure of LMR cathode electrode should be much less than that without TPFPB.

Direct evidence is provided by TEM analysis of the fresh and cycled electrodes in different electrolytes (Fig. 4). Before cycling, relative smooth particle surface is observed (Fig. 4a). After 300 cycles, clear difference in particle surfaces is identified for electrodes (recovered from duplicate cells) cycled in electrolyte without and with TPFPB. In baseline electrolyte (Fig. 4b), the image reveals a distinguishable passivation layer on the surface of cycled $Li[Li_{0.2}Ni_{0.2}Mn_{0.6}]O_2$ electrode, with a thickness of 10–15 nm. In comparison, electrode cycled in the presence of TPFPB (Fig. 4c and d) displays well maintained particle morphology with smooth particle surface covered by a much thinner passivation layer. These findings substantiate our hypothesis on the capability of TPFPB in modifying the interfacial reactions through the stabilization of anions/radicals as well as dissolution of oxygen species and insulating byproducts.

Fig. 5 compares the evolutions of charge/discharge curves and their corresponding dQ/dV plots of LMR cathode electrodes at different cycles without and with TPFPB additive. In the baseline cell, discharge curves show significant voltage decay with cycling (Fig. 5a). It is generally believed that the gradual phase transformation of Li_2MnO_3/MnO_2 component from layered to spinel leads to the voltage fading [37,38]. Considering the fact that LMR cathode has to be charged to high voltage of 4.6–4.8 V, the

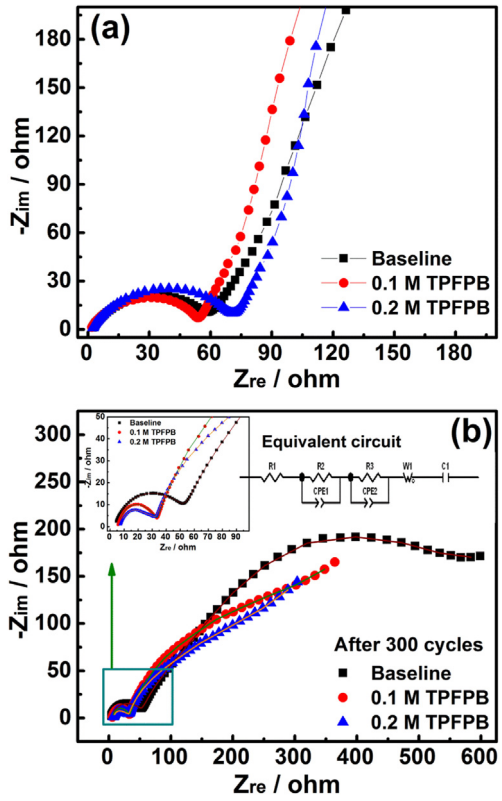

Fig. 6. Nyquist plots of the $Li[Li_{0.2}Ni_{0.2}Mn_{0.6}]O_2$ electrodes in electrolytes without and with TPFPB additive, (a) before cycling, (b) after 300 cycles. The insets of (b) present the magnified high-frequency semicircle and the equivalent circuit for spectra fitting.

instability of electrolyte at high voltage is worsened by the generation of O_2^{2-} and O_2 from the activation of Li_2MnO_3 component during charge. The unavoidable formation of passivation film covering cathode quickly and continuously increases the cell impedance and thus the electrode polarization of LMR cathode. In the presence of TPFPB (Fig. 5c and e), the voltage degradation is effectively alleviated because of the reduced thickness of passivation film, as proposed in Fig. 1.

More detailed information about the redox reactions is observed from their corresponding dQ/dV curves as presented in Fig. 5b, d and f. In accordance to the charge/discharge profiles, all the electrodes show gradual evolution of intercalation peak at ca. 2.9 V, due to the continuous formation of spinel phase in the electrode structure. It is worth to note that the peak intensity corresponding to spinel formation becomes much stronger after repeated cycling in electrolytes with TPFPB additive (Fig. 5d and e) than that in baseline electrolyte (Fig. 5b). This confirms our conclusion that TPFPB alleviates the cell impedance increase by tailoring the interfacial reactions without affecting the intrinsic structural transformation in the bulk material. In fact, it is because of the improved quality of passivation film on cathode after adding TPFPB,

Table 2
Fitted results of the EIS spectra for $Li[Li_{0.2}Ni_{0.2}Mn_{0.6}]O_2$ before and after cycling.

$Li[Li_{0.2}Ni_{0.2}Mn_{0.6}]O_2$		Baseline electrolyte	0.1 M TPFPB added	0.2 M TPFPB added
Before cycling ($R_{sf}+R_{ct}$)/Ω		63	57	74
After 300 cycles/Ω	R_{sf}	46	26	22
	R_{ct}	654	375	350

the reaction pathway from layered to spinel structure e.g. the continuous increase of 2.9 V peak (Fig. 5d and e) is still clearly visible even after 200 cycles. Similar effects can be found for LMR cathode by AlF_3 coating, which is unable to eliminate the layered-to-spinel phase transformation but effectively improve the cycling stability of LMR cathode materials by stabilizing the electrode/electrolyte interface [5,10]. The result further evidences that the voltage decay of LMR cathode materials is caused by an intrinsic lattice structure transformation and very little can be altered by electrolytes and/or additives. During de-intercalation process, for the cell with baseline electrolyte (Fig. 5b), the de-intercalation peaks in dQ/dV curves shift dramatically toward high voltage during cycling, indicating a large increase of electrode polarization because of the deteriorated electrode/electrolyte interface caused by the aggressive side reactions as discussed earlier. The deteriorated electrode/electrolyte interface is unfavorable for reversible/complete lithium ion intercalation/de-intercalation due to the increased kinetic barrier [39], resulting in continuous capacity degradation during cycling. On the contrary, with TPFPB, the de-intercalation peaks of $Li[Li_{0.2}Ni_{0.2}Mn_{0.6}]O_2$ show much less shift in dQ/dV curves during extended cycling (Fig. 5d and f) because of the improved stability of electrode/electrolyte interface which is favorable for reversible lithium ion intercalation/de-intercalation and thus promises the enhanced long-term cycling performance.

Electrochemical impedance spectroscopy was conducted to further confirm the functions of TPFPB additive. The impedance spectra measured before cycling and after 300 cycles are presented in Fig. 6a and b, in which a high-frequency semicircle, an intermediate-frequency semicircle and low-frequency tails are observed. Generally, the high-frequency semicircle is related to the resistance arising from the passivation surface film (R_{sf}) [5,40]. The intermediate-frequency semicircle is ascribed to the charge transfer resistance (R_{ct}) in the electrode/electrolyte interface. The low-frequency tail is associated with the Li^+ ion diffusion process in the solid electrode. The EIS spectra were fitted with the equivalent circuit [41,42] inset in Fig. 6b and the detailed results are summarized in Table 2. Before cycling, EIS spectra only show one semicircle ranging from high to medium frequency, which is composed of surface film resistance (minor) and charge transfer resistance (major). Slight difference is observed for cells before cycling except the one with 0.2 M TPFPB, which shows slightly higher interfacial resistance due to the increased viscosity and decreased conductivity (Table 1). After 300 cycles, electrode cycled in electrolyte with 0.2 M TPFPB additive exhibits a small surface layer resistance (22 Ω), only about half of that cycled in electrolyte without additive (46 Ω), indicating a thinner passivation film on the electrode surface. With 0.2 M TPFPB, the cell shows a charge transfer resistance of 350 Ω which is much smaller than that observed in baseline electrolyte (654 Ω). The stable interfacial resistances in the presence of TPFPB reflect an improved quality of electrode/electrolyte interface which reversibly allows the timely charge transfer. The EIS result is in good agreement with the previous electrochemical data discussion.

It is worth to note that the surface film formation and/or oxygen species evolution should continue during extended cycling even in the presence of TPFPB. The evolved oxygen species and the insoluble lithium salts in the surface film (Li_2O, LiF etc.) will further coordinate with TPFPB and reduce the content of free TPFPB in the electrolyte. Therefore, concentration of TPFPB is critically important to enable a sustaining operation of LMR cathode material. Difference is observed when the cells with different concentration of TPTPB were cycled to 500 cycles (Fig. 3b). The cell with higher concentration of TPTPB (0.2 M, 76.8% capacity retention after 500 cycles) appears to outperform the one with lower concentration of TPFPB (0.1 M, 74.2% capacity retention after 500 cycles). On this

basis, for cells with electrolyte containing same concentration of TPFPB, the cycling performance would be closely related with the amount of electrolyte, because higher amount of electrolyte contains higher content of TPFPB which could coordinate with more oxygen species and other insoluble byproducts. In addition, for electrodes with higher loading, both the amount of electrolyte and the concentration of TPFPB should be further optimized prior to practical applications in order to achieve good long-term cycling performance.

4. Conclusions

The anion receptor TPFPB has been demonstrated to be a promising additive to improve the long-term cycling performance of LMR cathode $Li[Li_{0.2}Ni_{0.2}Mn_{0.6}]O_2$. As an effective anion receptor, TPFPB captures the intermediate oxygen anions or radicals released from structural lattice during the activation of Li_2MnO_3 component. The increased oxygen solubility in the presence of perfluorinated compounds also prevents the oxygen from direct contact with carbonate solvents, greatly suppressing the side reactions. In addition, other byproducts formed at high voltages after each cycle, especially the insulating LiF, are also partially soluble in the presence of TPFPB. Therefore, the passivation film accumulated from various paths on the cathode surface is largely alleviated as confirmed by TEM characterization, impedance measurement and electrochemical data analysis. This work also implies that in addition to the intrinsic layered-to-spinel phase transformation, interfacial reactions also significantly affect the electrode polarization, which aggravates the voltage hysteresis, and the capacity degradation of LMR cathodes. Basic understanding and modification on the interface reactions on LMR cathode surface are necessary toward the development of high-energy layered composite cathodes for advanced lithium ion batteries.

Acknowledgments

This work was supported by the Assistant Secretary for Energy Efficiency and Renewable Energy, Office of Vehicle Technologies of the U. S. Department of Energy (DOE) under Contract No. DE-AC02-05CH11231, Subcontract No. 18769, under the Batteries for Advanced Transportation Technologies program. The microscopic study described in this paper was conducted in the William R. Wiley Environmental Molecular Sciences Laboratory (EMSL), a national scientific user facility sponsored by DOE's Office of Biological and Environmental Research and located at Pacific Northwest National Laboratory (PNNL). PNNL is operated by Battelle for the DOE under Contract DE-AC05-76RLO1830.

References

[1] J. Zheng, J. Xiao, W. Xu, X. Chen, M. Gu, X. Li, J.-G. Zhang, J. Power Sources 227 (2013) 211.
[2] J. Zheng, J. Xiao, Z. Nie, J.-G. Zhang, J. Electrochem. Soc. 160 (2013) A1264.
[3] M.M. Thackeray, C.S. Johnson, J.T. Vaughey, N. Li, S.A. Hackney, J. Mater. Chem. 15 (2005) 2257.
[4] M.M. Thackeray, S.-H. Kang, C.S. Johnson, J.T. Vaughey, R. Benedek, S.A. Hackney, J. Mater. Chem. 17 (2007) 3112.
[5] J.M. Zheng, Z.R. Zhang, X.B. Wu, Z.X. Dong, Z. Zhu, Y. Yang, J. Electrochem. Soc. 155 (2008) A775.
[6] H. Yu, H. Zhou, J. Phys. Chem. Lett. 4 (2013) 1268.
[7] A.R. Armstrong, M. Holzapfel, P. Novák, C.S. Johnson, S.-H. Kang, M.M. Thackeray, P.G. Bruce, J. Am. Chem. Soc. 128 (2006) 8694.
[8] M. Gu, I. Belharouak, A. Genc, Z. Wang, D. Wang, K. Amine, F. Gao, G. Zhou, S. Thevuthasan, D.R. Baer, J.-G. Zhang, N.D. Browning, J. Liu, C. Wang, Nano Lett. 12 (2012) 5186.
[9] J.M. Zheng, J. Li, Z.R. Zhang, X.J. Guo, Y. Yang, Solid State Ionics 179 (2008) 1794.
[10] M. Gu, I. Belharouak, J. Zheng, H. Wu, J. Xiao, A. Genc, K. Amine, S. Thevuthasan, D.R. Baer, J.-G. Zhang, N.D. Browning, J. Liu, C. Wang, ACS Nano 7 (2013) 760.
[11] A. Ito, D. Li, Y. Sato, M. Arao, M. Watanabe, M. Hatano, H. Horie, Y. Ohsawa, J. Power Sources 195 (2010) 567.
[12] J. Zheng, M. Gu, J. Xiao, P. Zuo, C. Wang, J.-G. Zhang, Nano Lett. 13 (2013) 3824.
[13] N. Yabuuchi, K. Yoshii, S.-T. Myung, I. Nakai, S. Komaba, J. Am. Chem. Soc. 133 (2011) 4404.
[14] S.A. Freunberger, Y. Chen, N.E. Drewett, L.J. Hardwick, F. Bardé, P.G. Bruce, Angew. Chem. Int. Ed. 50 (2011) 8609.
[15] J. Xiao, J. Hu, D. Wang, D. Hu, W. Xu, G.L. Graff, Z. Nie, J. Liu, J.-G. Zhang, J. Power Sources 196 (2011) 5674.
[16] B. Markovsky, A. Rodkin, G. Salitra, Y. Talyosef, D. Aurbach, H.-J. Kim, J. Electrochem. Soc. 151 (2004) A1068.
[17] R. Dedryvère, H. Martinez, S. Leroy, D. Lemordant, F. Bonhomme, P. Biensan, D. Gonbeau, J. Power Sources 174 (2007) 462.
[18] A.D. Robertson, P.G. Bruce, Chem. Mater. 15 (2003) 1984.
[19] J.M. Zheng, X.B. Wu, Y. Yang, Electrochim. Acta 56 (2011) 3071.
[20] S. Tan, Z. Zhang, Y. Li, Y. Li, J. Zheng, Z. Zhou, Y. Yang, J. Electrochem. Soc. 160 (2013) A285.
[21] Z. Chen, K. Amine, J. Electrochem. Soc. 153 (2006) A1221.
[22] K.Y. Chung, H.S. Lee, W.-S. Yoon, J. McBreen, X.-Q. Yang, J. Electrochem. Soc. 153 (2006) A774.
[23] X. Sun, H.S. Lee, X.Q. Yang, J. McBreen, Electrochem. Solid-state Lett. 4 (2001) A184.
[24] X. Sun, H.S. Lee, X.-Q. Yang, J. McBreen, Electrochem. Solid-state Lett. 5 (2002) A248.
[25] M. Herstedt, M. Stjerndahl, T. Gustafsson, K. Edström, Electrochem. Commun. 5 (2003) 467.
[26] J. Zheng, D. Zhu, Y. Yang, Y. Fung, Electrochim. Acta 59 (2012) 14.
[27] W. Xu, X. Chen, F. Ding, J. Xiao, D. Wang, A. Pan, J. Zheng, X.S. Li, A.B. Padmaperuma, J.-G. Zhang, J. Power Sources 213 (2012) 304.
[28] L.F. Li, H.S. Lee, H. Li, X.Q. Yang, K.W. Nam, W.S. Yoon, J. McBreen, X.J. Huang, J. Power Sources 184 (2008) 517.
[29] N.-S. Choi, G. Jeong, B. Koo, Y.-W. Lee, K.T. Lee, J. Power Sources 225 (2013) 95.
[30] F. De Giorgio, F. Soavi, M. Mastragostino, Electrochem. Commun. 13 (2011) 1090.
[31] Y. Wang, D. Zheng, X.-Q. Yang, D. Qu, Energy Environ. Sci. 4 (2011) 3697.
[32] J.G. Riess, M. Le Blanc, Angew. Chem. Int. Ed. 17 (1978) 621.
[33] B. Xie, H.S. Lee, H. Li, X.Q. Yang, J. McBreen, L.Q. Chen, Electrochem. Commun. 10 (2008) 1195.
[34] R. Diaz-Torres, S. Alvarez, Dalton Trans. 40 (2011) 10742.
[35] Z. Lu, J.R. Dahn, J. Electrochem. Soc. 149 (2002) A815.
[36] S.H. Kang, M.M. Thackeray, J. Electrochem. Soc. 155 (2008) A269.
[37] C.S. Johnson, N. Li, C. Lefief, J.T. Vaughey, M.M. Thackeray, Chem. Mater. 20 (2008) 6095.
[38] B. Xu, C.R. Fell, M. Chi, Y.S. Meng, Energy Environ. Sci. 4 (2011) 2223.
[39] J. Zheng, W. Shi, M. Gu, J. Xiao, P. Zuo, C. Wang, J.-G. Zhang, J. Electrochem. Soc. 160 (2013) A2212.
[40] F. Nobili, F. Croce, B. Scrosati, R. Marassi, Chem. Mater. 13 (2001) 1642.
[41] Y.J. Kang, J.H. Kim, S.W. Lee, Y.K. Sun, Electrochim. Acta 50 (2005) 4784.
[42] J. Zheng, X. Wu, Y. Yang, Electrochim. Acta 105 (2013) 200.